Auxin transport inhibitors impair vesicle motility and actin cytoskeleton dynamics in diverse eukaryotes

Pankaj Dhonukshe[a,b,c], Ilya Grigoriev[d], Rainer Fischer[e], Motoki Tominaga[f,g], David G. Robinson[h], Jiří Hašek[i], Tomasz Paciorek[a,j], Jan Petrášek[k], Daniela Seifertová[k], Ricardo Tejos[l,m], Lee A. Meisel[m], Eva Zažímalová[k], Theodorus W. J. Gadella, Jr.[b], York-Dieter Stierhof[a], Takashi Ueda[n], Kazuhiro Oiwa[f], Anna Akhmanova[d], Roland Brock[e,o], Anne Spang[p,q], and Jiří Friml[a,l,r,s]

[a]Zentrum für Molekularbiologie der Pflanzen (ZMBP), Universität Tübingen, Auf der Morgenstelle 3, D-72076 Tübingen, Germany; [d]Department of Cell Biology and Genetics, Erasmus Medical Centre, P.O. Box 1738, 3000 DR Rotterdam, The Netherlands; [e]Institute for Cell Biology, University of Tübingen, D-72076 Tübingen, Germany; [f]Kansai Advanced Research Centre, National Institute of Information and Communications Technology, Kobe 651-2492, Japan; [h]Cell Biology, Heidelberg Institute for Plant Sciences, University of Heidelberg, D-69120 Heidelberg, Germany; [i]Institute of Microbiology, Academy of Sciences of the Czech Republic, Vídeňská 1083, 142 20 Prague 4, Czech Republic; [b]Section of Molecular Cytology, Swammerdam Institute for Life Sciences, University of Amsterdam, 1098 SM Amsterdam, The Netherlands; [k]Institute of Experimental Botany, Academy of Sciences of the Czech Republic, Rozvojová 263, 165 02 Praha 6, Czech Republic; [n]Department of Biological Sciences, Graduate School of Science, University of Tokyo, 7-3-1 Hongo, Bunkyo-ku, Tokyo 113-0033, Japan; [p]Friedrich Miescher Laboratory of the Max Planck Society, Spemannstrasse 39, D-72076 Tübingen, Germany; [r]Department of Functional Genomics, Masaryk University, Kamenice 25, C2-62500 Brno, Czech Republic; [l]Department of Plant Systems Biology, Flanders Institute for Biotechnology and Department of Molecular Genetics, Ghent University, Technologiepark 927, 9052 Gent, Belgium; and [m]Millennium Nucleus in Plant Cell Biology and Center of Plant Biotechnology, Andrés Bello University, Avenue República 217, 837-0146, Santiago, Chile

Edited by Joanne Chory, Salk Institute for Biological Studies, La Jolla, CA, and approved January 22, 2008 (received for review December 6, 2007)

Many aspects of plant development, including patterning and tropisms, are largely dependent on the asymmetric distribution of the plant signaling molecule auxin. Auxin transport inhibitors (ATIs), which interfere with directional auxin transport, have been essential tools in formulating this concept. However, despite the use of ATIs in plant research for many decades, the mechanism of ATI action has remained largely elusive. Using real-time live-cell microscopy, we show here that prominent ATIs such as 2,3,5-triiodobenzoic acid (TIBA) and 2-(1-pyrenoyl) benzoic acid (PBA) inhibit vesicle trafficking in plant, yeast, and mammalian cells. Effects on micropinocytosis, rab5-labeled endosomal motility at the periphery of HeLa cells and on fibroblast mobility indicate that ATIs influence actin cytoskeleton. Visualization of actin cytoskeleton dynamics in plants, yeast, and mammalian cells show that ATIs stabilize actin. Conversely, stabilizing actin by chemical or genetic means interferes with endocytosis, vesicle motility, auxin transport, and plant development, including auxin transport-dependent processes. Our results show that a class of ATIs act as actin stabilizers and advocate that actin-dependent trafficking of auxin transport components participates in the mechanism of auxin transport. These studies also provide an example of how the common eukaryotic process of actin-based vesicle motility can fulfill a plant-specific physiological role.

PIN proteins | plant development | vesicle traffic | auxin efflux inhibitors

The signaling molecule auxin plays a pivotal role in regulating plant development; however, auxin is unique among plant hormones because it is transported in a directional (polar) manner through plant tissues (1). This polar transport mediates an asymmetric distribution of auxin between cells that triggers a plethora of growth and developmental processes, such as embryo and organ development, vascular patterning, apical dominance, and tropisms (2–6). Our knowledge of the mechanism of polar auxin transport and its role in plant development has largely been based on pharmacological tools: auxin transport inhibitors (ATIs) that have been in use for more than half a century. ATIs such as 1-naphthylphthalamic acid (NPA), 2,3,5-triiodobenzoic acid (TIBA), and 2-(1-pyrenoyl) benzoic acid (PBA) inhibit auxin efflux and thus block polar auxin movement between cells (7, 8). Exogenously applied ATIs interfere with auxin distribution and thus perturb plant development (1). Similar developmental defects identified in some *Arabidopsis* mutants have led to the identification of the auxin efflux and influx components PIN (5, 9) and AUX1/LAX (10, 11) proteins, respectively. PIN proteins have been shown, on account of their polar, subcellular localization, to direct the polar flow of auxin (12). Inhibition of ADP-ribosylation factor (ARF) guanine nucleotide exchange factor (GEF)-dependent vesicle trafficking by brefeldin A also has suggested that both PIN and AUX1 auxin carriers undergo constitutive cycling between the plasma membrane (PM) and endosomes (13–15). Unexpectedly, ATIs such as TIBA or PBA interfere with this trafficking (13, 15), but the underlying cellular mechanism and functional significance of this effect is unclear. Here, we demonstrate that TIBA and PBA interfere with actin dynamics in plants and also in yeast and mammalian cells providing a mechanism by which these drugs disrupt vesicle subcellular trafficking, including that of PIN auxin efflux carriers.

Results

Supporting Information (SI). For further information on the results discussed below, see SI Figs. 5–15, SI Movies 1–14, and *SI Results*.

ATIs Interfere with Multiple Vesicle Trafficking Processes in Plant Cells. To address the mechanism of ATIs effect on auxin carrier trafficking, we explored their effects on various vesicle trafficking processes by real-time live-cell microscopy. First we tested the effect of ATIs on endocytic, endosomal, and Golgi dynamics in suspension-cultured tobacco BY-2 cells and in *Arabidopsis* root cells. FM4–64 was used as an endocytic tracer (16), GFP-Ara7 (the plant ortholog of mammalian Rab5) (17) was used as an endosomal

Author contributions: P.D., L.A.M., E.Z., T.W.J.G., K.O., A.A., R.B., A.S., and J.F. designed research; P.D., I.G., R.F., M.T., J.H., T.P., J.P., D.S., R.T., Y.-D.S., T.U., A.A., and A.S. performed research; D.G.R. contributed new reagents/analytic tools; P.D., I.G., R.F., M.T., J.H., J.P., E.Z., Y.-D.S., T.U., A.A., R.B., and A.S. analyzed data; and P.D. and J.F. wrote the paper.

The authors declare no conflict of interest.

This article is a PNAS Direct Submission.

[c]Present address: Molecular Genetics Group, Department of Biology, Utrecht University, Padualaan 8, 3584 CH, Utrecht, The Netherlands.

[g]Present address: Discovery Research Institute, RIKEN, 2-1, Hirosawa, Wako, Saitama 351-0198, Japan.

[j]Present address: Stanford University, 371 Serra Mall, Stanford, CA 94305-5020.

[o]Present address: Department of Biochemistry, Nijmegen Centre for Molecular Life Sciences, Radboud University Nijmegen Medical Centre, Geert Grooteplein 28, 6525 GA, Nijmegen, The Netherlands.

[q]Present address: Biozentrum, University of Basel, Klingelbergstrasse 50/70, CH-4056 Basel, Switzerland.

[s]To whom correspondence should be addressed. E-mail: jiri.friml@psb.ugent.be.

This article contains supporting information online at www.pnas.org/cgi/content/full/0711414105/DC1.

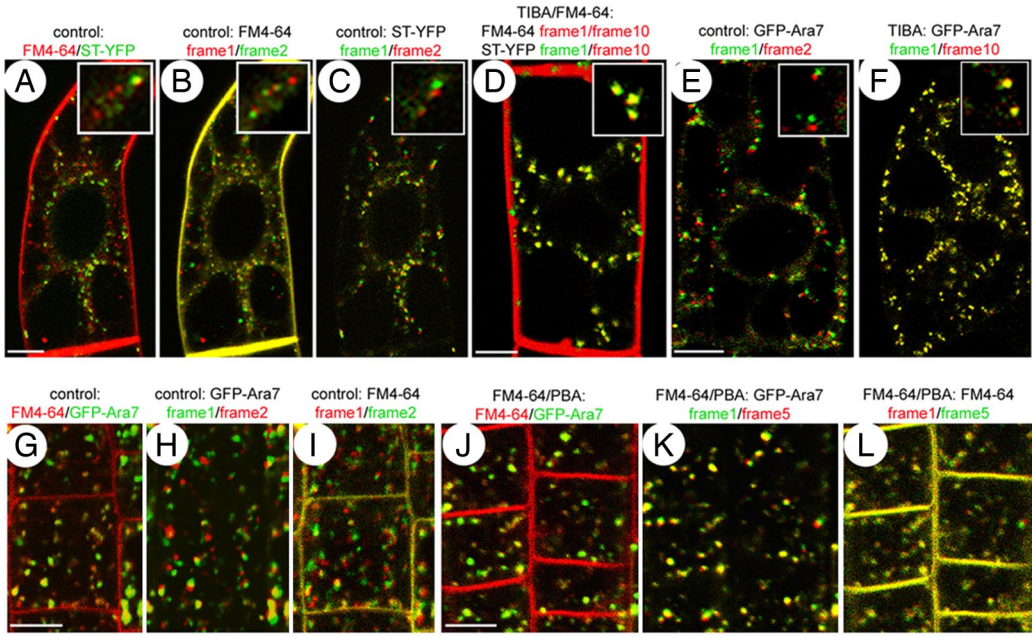

Fig. 1. Effects of ATIs on endocytosis and vesicle motility in plant cells. (*A–F*) Endocytosis and endosomal and *trans*-Golgi motility in tobacco BY-2 cells as visualized by FM4-64 (red), ST-YFP (green), and GFP-Ara7 (green). Solvent control, FM4-64 (2 μM, 30 min): FM4-64/ST-YFP overlay (*A*), FM4-64 overlay of frame 1 (red) on frame 2 (+3 s, green) (*B*), ST-YFP overlay of frame 1 (green) on frame 2 (+3 s, red) (*C*). (*D*) TIBA (25 μM, 30 min) followed by TIBA/FM4–64 (90 min): FM4–64 (red), ST-YFP overlay of frame 1 (green) on frame 10 (+30 s, red). (*E*) Solvent control (30 min), GFP-Ara7 overlay of frame 1 (green) on frame 2 (+1.5 s, red). (*F*) Treatment with TIBA (25 μM, 30 min), GFP-Ara7 overlay of frame 1 (green) on frame 10 (+15 s, red). Note the *Insets* for better visualization of vesicles. (Scale bars: 5 μm.) (*G–L*) Endocytosis and endosomal motility in *Arabidopsis* root cells as visualized by FM4-64 (red) and GFP-Ara7 (green). Solvent control, FM4-64 (2 μM, 30 min): FM4-64/GFP-Ara7 overlay (*G*). GFP-Ara7 overlay of frame 1 (green) on frame 2 (+6 s, red) (*H*), FM4-64 overlay of frame 1 (red) on frame 2 (+6 s, green) (*I*). FM4-64 (2 μM, 30 min) followed by PBA (15 μM)/FM4-64 (30 min): FM4-64/GFP-Ara7 overlay (*J*), GFP-Ara7 overlay of frame 1 (green) on frame 5 (+30 s, red) (*K*), FM4-64 overlay of frame 1 (red) on frame 5 (+30 s, green) (*L*). (Scale bars: 5 μm.)

marker, and sialyl transferase-yellow fluorescent protein (ST-YFP) (18) was used as a Golgi marker. In BY-2 cells, FM4–64 was internalized within 5–10 min, and labeled endosomes, which were largely distinct from the ST-YFP-labeled Golgi (Fig. 1*A*). Both endosomes and Golgi displayed a highly dynamic behavior, which was visualized through superimposition of two successive frames (3-s interval between frames; color-coded red and green) for FM4–64 (Fig. 1*B*) and ST-YFP (Fig. 1*C*). TIBA (25 μM) blocked FM4–64 endocytosis, and Golgi and endosomal movements in BY-2 cells (Fig. 1 *D–F* and SI Movies 1 and 2). Similar effects were observed in *Arabidopsis* with TIBA (25 μM, data not shown) and PBA (15 μM) (SI Movies 3 and 4, Fig. 1 *G–L*, *SI Results Part 1*, and SI Fig. 6 *D–G*). The lowest effective concentrations showing noticeable effects were 5 μM for TIBA and 1 μM for PBA. Several controls for the specific effect of ATIs on subcellular motility were performed (*SI Results Part 2*). Structurally related acidic compounds such as benzoic acid (BeA) did not affect endocytosis or vesicle motility (SI Movie 5). The effects of ATIs did not include general perturbations in cellular ultrastructure (SI Fig. 6 *H* and *I*) and were completely reversible (SI Fig. 6 *A–C*). In summary, these results show that some ATIs such as TIBA and PBA block vesicle and organelle motility in plant cells.

ATIs Interfere with Endocytosis and Endosomal Dynamics in Nonplant Systems. Because mechanisms of many basic cellular processes, including that of endocytosis (14) or vesicle motility, are conserved between plants and other eukaryotes, we also investigated effects of ATIs in yeast and mammalian cells. First we probed endocytosis in the budding yeast *Saccharomyces cerevisiae* by analyzing the uptake of FM4–64. Within 60 min after its application, internalized FM4–64 labeled the endocytic pathway (19) and ultimately localized to the vacuolar membrane (Fig. 2*A*). When yeast cells were pretreated with PBA (90 μM) or TIBA (100 μM, data not shown), FM4–64 uptake was reduced and FM4–64 persisted to large extent at the PM (Fig. 2*B*). We also tested the effects of ATIs on mammalian cells. Three main types of endocytosis can be distinguished in HeLa cells: macropinocytosis, which is strongly dependent on actin cytoskeleton dynamics; clathrin-mediated endocytosis; and lipid raft/caveolar-dependent endocytosis (20). We tested the effects of TIBA and PBA on all three types of endocytosis by monitoring their effects on the uptake of fluorescently labeled dextran, transferrin, and the cholera toxin subunit B, which serve as specific markers for these pathways, respectively (20). TIBA and PBA mostly affected the uptake and intracellular distribution of the macropinocytosis marker dextran (Fig. 2 *C–H*) as confirmed by quantification using flow cytometry (Fig. 2*I*). The preferential inhibition of macropinocytosis (which depends largely on actin dynamics) (20) provided a hint that ATIs might affect some actin-related process.

We then analyzed the dynamics of GFP-Rab5-labeled endosomes in HeLa cells (21). In control cells, the distribution of GFP-Rab5-positive structures gradually decreased from the cell periphery toward the cell center and showed a second peak near the nucleus (Fig. 2*J*). Individual vesicles moved slowly at the periphery of the cell but switched to a fast movement in the internal regions (21). TIBA and PBA slowed down Rab5 dynamics preferentially at the cell margins, causing an accumulation of Rab5 in these areas, and as a result the ratio of peripheral versus central Rab5 localization increased (SI Movie 6 and Fig. 2 *K* and *L*). Because the peripheral movement of endosomes depends primarily on the actomyosin system, whereas the fast movement in the central regions is mostly microtubule-based (22), the preferential effect of ATIs on the endosomes at the periphery further substantiated the results above that ATIs may affect the actin cytoskeleton.

PBA and TIBA also showed pronounced effects on cellular behavior and morphology in both yeast (SI Fig. 13) and mammalian

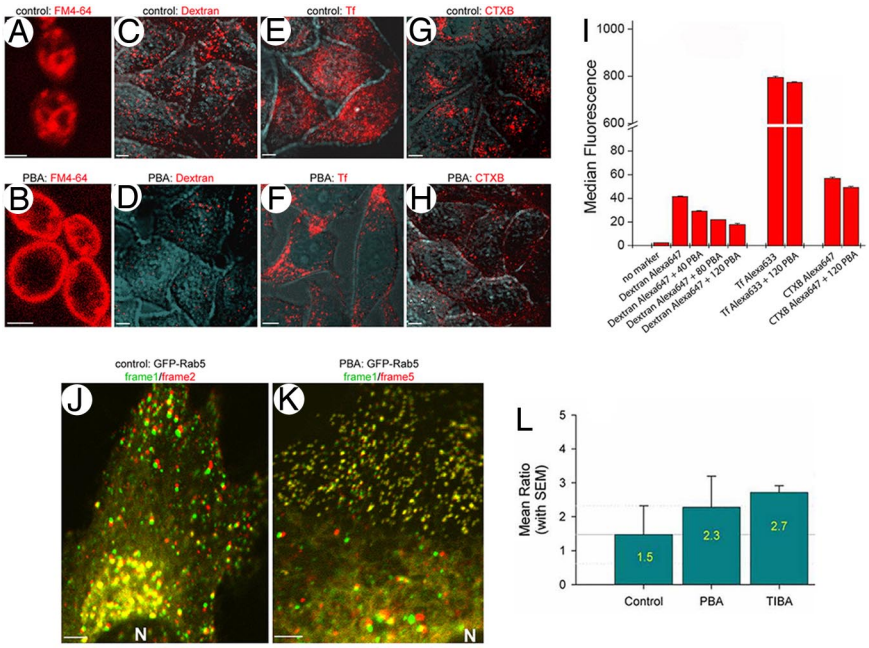

Fig. 2. Effects of ATIs on endocytosis and vesicle motility in yeast and mammalian cells. (*A* and *B*) Effect of PBA on endocytosis in yeast as visualized by FM4-64 (red) uptake. (*A*) Solvent control (30 min) followed by FM4-64 (2 μM, 60 min). (*B*) PBA (90 μM, 30 min) followed by PBA/FM4-64 (60 min). (Scale bars: 2 μm.) (*C–H*) Effect of PBA on different types of endocytosis in HeLa cells as visualized by different markers (red). Differential interference contrast (DIC) images (light blue) are merged with fluorescent images (red). (*C–H*) HeLa cells treated with solvent (30 min, *C*, *E*, and *G*) or PBA (80 μM, 30 min, *D*, *F*, and *H*) followed by incubation with dextran–Alexa Fluor 647 (5 μM, *C* and *D*), transferrin (Tf)–Alexa Fluor 633 (25 μg/ml, *E* and *F*), and cholera toxin B subunit (CTXB)–Alexa Fluor 647 (10 μg/ml, *G* and *H*) at 37°C (30 min). (Scale bars: 5 μm.) (*I*) Quantitative FACS analysis showing dose-dependent effect of PBA on macropinocytosis, clathrin-mediated endocytosis, and caveolar endocytosis. (Scale bars: 5 μm.) PBA concentration is in μM. (*J–L*) Effect of PBA on endosomal motility and distribution in HeLa cells as visualized by GFP-Rab5. (*J*) Solvent control (30 min), GFP-Rab5 overlay of frame 1 (green) on frame 2 (+2 s, red). (*K*) Treatment with PBA (60 μM, 30 min), GFP-Rab5 overlay of frame 1 (green) on frame 5 (+10 s, red). N indicates the nucleus of the cell. (Scale bars: 2 μm.) (*L*) Plots showing the ratio of the mean GFP-Rab5 fluorescence intensity in the peripheral (4 μm near the cell margin) versus internal (10 μm away from the cell edge) cell regions as a measure of the distribution of Rab5-positive endosomes.

(fibroblast and HeLa) cells, including changes in cell shape, defects in chromosome separation, and a delay in cell division (SI Fig. 12 *A–C*). These phenotypes correspond well with other studies showing a requirement of the actin cytoskeleton for cell shape and cell division (23, 24).

ATIs Inhibit Actin Dynamics in Yeast, Mammalian, and Plant Cells. Next, we tested the effect of ATIs on fibroblast monolayer wound healing, which is a standard assay for actin-related defects (25). Movement of control fibroblasts into the wound results in its complete closure within 16 h (SI Fig. 7*A*). In contrast, cells treated with PBA or TIBA failed to close a wound of the same width (SI Fig. 7*B*), demonstrating a defect in fibroblast mobility (*SI Results Part 3* and SI Fig. 7 *C–F*). Because locomotion of mammalian fibroblasts depends strictly on a dynamic actin cytoskeleton (25), this further indicated that ATIs affect an actin-related process.

Myosin motor proteins are involved in vesicle traffic and actin dynamics (26) and could be the direct target of ATIs. Therefore, we tested the effect of TIBA and PBA on the function of mammalian (Myosin II) and plant (Myosin XI) myosin motors (26). In the *in vitro* actin/myosin motility assay, we found no effect of TIBA and PBA on the function of these motors (SI Fig. 10), excluding these motor proteins as a direct molecular target of ATIs.

Next, we examined the effect of ATIs on the actin cytoskeleton itself. We investigated actin cytoskeleton dynamics *in vivo* using cells expressing GFP-actin (27). ATIs induced enhanced stress fiber formation in both HeLa cells and fibroblasts and dramatically decreased the dynamics of actin cytoskeleton (SI Movies 7 and 8 and Fig. 3 *A* and *B*). Next, we analyzed the actin cytoskeleton in yeast. Actin was visualized by actin immunolocalization in fixed cells (Fig. 3 *G* and *H*) or by using the actin-binding protein 140-GFP (ABP140-GFP) (28) in living cells (Fig. 3 *I–K*). Both methods showed that, compared with controls (Fig. 3 *G* and *I*), TIBA and PBA (Fig. 3 *H* and *J*), but not BeA (SI Fig. 15), induced patching of actin, which is a characteristic feature of actin stabilization (28). This effect of ATIs was entirely different from the one induced by the well known actin-depolymerizing drug latrunculin A (28), which leads to a cytosolic distribution of ABP140-GFP (Fig. 3*K*). These observations from mammalian and yeast cells strongly indicate that ATIs cause hyperstabilization of actin.

To test whether ATIs also exhibit the same effects on actin dynamics in plants, we used an actin marker consisting of the second actin-binding domain of Fimbrin tagged to GFP (GFP-Fimbrin) for visualizing actin *in vivo* (29). Similar to the effects observed in mammalian cells, TIBA treatment led to the formation of thick actin bundles in tobacco BY-2 cells compared with control cells (Fig. 3 *C* and *D*). Similarly, in *Arabidopsis* root cells, TIBA and PBA (SI Movies 9 and 10 and Fig. 3 *E* and *F*), but not BeA (SI Movie 11), affected the actin cytoskeleton by inducing its bundling and slowing down its dynamics. To confirm whether the effects of ATIs on the actin cytoskeleton are related to stabilization of actin filaments, we tested their effects after depolymerizing actin filaments with latrunculin B (30). In *Arabidopsis*, treatment with latrunculin B depolymerized actin filaments (visualized by GFP-Fimbrin) and induced small aggregations of GFP-Fimbrin (compare SI Fig. 8 *A* and *B*). However, when cells were pretreated with jasplakinolide, an established actin cytoskeleton stabilizer in mammalian and yeast cells (31), actin filaments largely remained intact without being depolymerized (SI Fig. 8*C*). Similarly, PBA and TIBA kept actin filaments intact and in a bundled form, even in the presence of latrunculin B (SI Fig. 8 *D* and *E*). The effect of ATIs on actin dynamics does not seem to be direct, because actin

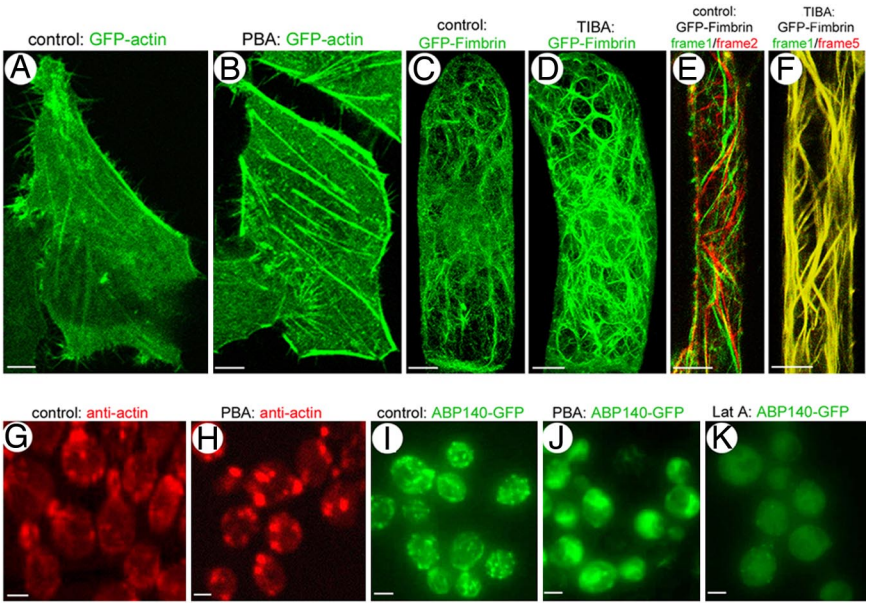

Fig. 3. Effects of ATIs on actin filaments in plant, yeast, and mammalian cells. (*A* and *B*) Effect of ATIs on GFP-actin expressing live HeLa cells. Solvent (30 min, *A*), and PBA (60 μM, 30 min, *B*). (Scale bars: 5 μm.) (*C* and *D*) Effect of ATIs on GFP-Fimbrin expressing live tobacco BY-2 cells. Solvent (30 min, *C*) and TIBA (25 μM, 30 min, *D*). (Scale bars: 5 μm.) (*E* and *F*) Effect of ATIs on GFP-Fimbrin expressing live *Arabidopsis* root cells. Solvent (30 min, *E*) and TIBA (25 μM, 30 min, *F*). GFP-Fimbrin overlay of frame 1 (green) on frame 2 (+3 s, red) (*E*) and GFP-Fimbrin overlay of frame 1 (green) on frame 5 (+15 s, red) (*F*). (Scale bars: 5 μm.) (*G*–*K*) Effect of ATIs on actin in yeast visualized by anti-actin immunolabeling (*G* and *H*) or in live yeast cells expressing ABP140-GFP (*I*–*K*). (*G* and *H*) Solvent (30 min, *G*) and PBA (90 μM, 30 min, *H*). (*I*–*K*) Solvent (120 min, *I*), PBA (50 μM, 120 min, *J*), and latrunculin A (10 μM, 30 min, *K*). (Scale bars: 2 μm.)

polymerization *in vitro* is unaffected by TIBA or PBA (SI Fig. 11). Therefore, we hypothesize that ATIs work either by activating an actin filament stabilizing factor or by inactivating an actin filament depolymerizing factor. Our results show that ATIs stabilize the actin cytoskeleton in diverse eukaryotic cells, providing a comprehensive explanation for the effects of ATIs on endocytosis and vesicle trafficking.

Actin Stabilization and ATIs Action Show Overlapping Cellular and Physiological Effects. The important question still remaining is whether the effects of ATIs on actin dynamics are linked to their physiological effects on auxin transport and auxin-related plant development. To address this question, we inhibited actin dynamics by using the actin stabilizer jasplakinolide. In plants, this compound showed overlapping effects on vesicle motility (SI Movie 12), FM4–64 uptake, and actin bundling (Fig. 4 *A* and *B*) to those observed for ATIs.

Next, we grew *Arabidopsis* plantlets on TIBA- or jasplakinolide-supplemented medium. The effects of TIBA and jasplakinolide on seedling development were similar and included defects in root growth, lateral root formation, and gravitropic response (Fig. 4 *C* and *D*). These developmental aberrations are typical for the inhibition of polar auxin transport and also can be detected in auxin transport mutants (1). Jasplakinolide induced a broader spectrum of defects, including a more general inhibition of plant growth. Similar but less pronounced developmental defects (SI Fig. 9*B*) also were found in transgenic *Arabidopsis* lines, in which the actin interacting protein 1 (AIP1) was conditionally silenced by RNAi. In these lines, AIP1 silencing induced the hyperstabilization of actin filaments (32) and the inhibition of FM4–64 uptake (SI Fig. 9*A*). Because AIP1 silencing takes a long time (at least 2–3 days) (32), we were unable to probe any short-term effects of this genetically stabilized actin cytoskeleton. Nevertheless, the long-term developmental consequences of actin-stabilization also included defects in root growth and gravitropism (SI Fig. 9*B*). Thus, both pharmacological and genetic stabilization of the actin cytoskeleton show broader but overlapping effects on plant development when compared with ATIs.

It is well established that ATIs act on plant development by disrupting the asymmetric auxin distribution, and that this effect can be indirectly visualized *in vivo* by auxin-responsive promoter-based reporters such as *DR5rev*::*GFP* (2, 4, 33). We tested the effects of actin filament stabilization on asymmetric DR5 activity during the gravitropic response (5). To induce gravity stimulation, we reoriented the seedlings by turning the plates by 135°. Seedlings on control plates and on plates supplemented with BeA (50 μM) displayed an asymmetric *DR5rev*::*GFP* signal at the lower side of the root tip accompanied with strong root bending within 4 h after change of the gravity vector (Fig. 4*E* and SI Fig. 9 *C* and *G*). However, in the case of jasplakinolide (5 μM), TIBA (5 μM), and PBA (1 μM) treatments, no establishment of the asymmetric *DR5rev*::*GFP* signal was detected, and the root gravitropic response was inhibited while root growth still occurred (Fig. 4 *F* and *G* and SI Fig. 9 *D*–*F*). Also, other instances of *DR5*-monitored asymmetric auxin distribution, such as in primary and secondary root meristems (2, 33), were affected by jasplakinolide (data not shown), which suggests that actin stabilizer jasplakinolide, similar to ATIs, interferes with asymmetric auxin distribution.

Actin Stabilization Blocks Subcellular PIN Dynamics and Inhibits Auxin Efflux. ATIs are known to interfere with polar auxin transport by inhibiting auxin efflux (34). To explore further the common physiological effects of ATIs and actin stabilizers, we tested the effects of actin stabilization on cellular auxin efflux. The accumulation of the PM-permeable synthetic auxin 1-naphthalene acetic acid (NAA) inside cultured cells gives a measure of active auxin efflux and circumvents the complexity of multicellular tissues (9). In cultured *Arabidopsis* cells, TIBA (Fig. 4*H*) and PBA (data not shown) as well as jasplakinolide (Fig. 4*H*) increased saturable accumulation of labeled NAA, but not of BeA, pointing to an inhibitory effect of these compounds on auxin efflux. Thus, jasplakinolide, similar to TIBA and PBA albeit to a lesser extent, inhibits auxin, suggesting a link between actin dynamics and auxin efflux.

What could that link be? One possibility is the subcellular targeting of PIN auxin efflux carriers. The pronounced inhibitory effect of the secretion and recycling inhibitor brefeldin A on auxin efflux has been rationalized in terms of the depletion of auxin efflux carriers from the PM (35). In contrast to brefeldin A, neither jasplakinolide (data not shown), PBA, nor TIBA visibly interfered with the PM localization of PIN1 (13, 36) or other auxin efflux proteins such as PGP1 and PGP19 in *Arabidopsis* roots (SI Fig. 14). Similarly, localization of PIN1-GFP in BY-2 cells also was unaffected by such treatments (Fig. 4 *I* and *J*), where ATI-sensitive, PIN-dependent auxin efflux has been extensively demonstrated (9). In contrast, the pronounced subcellular dynamics of PIN-

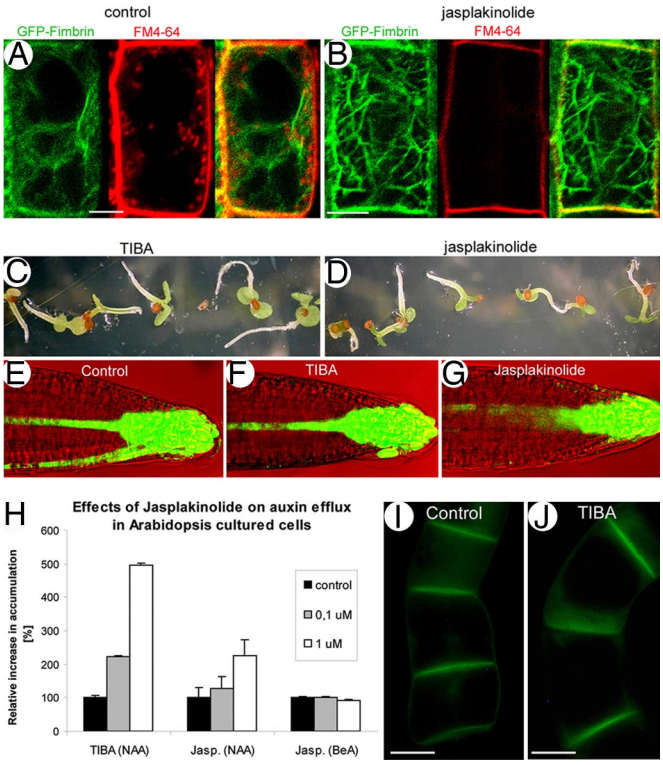

Fig. 4. Effect of actin stabilization on endocytosis, plant development, asymmetric auxin distribution, and auxin efflux. (*A* and *B*) Endocytosis of FM4-64 (2 μM, 30 min). Pretreatment and cotreatment with solvent (1 h, *A*) and jasplakinolide (10 μM, 1 h, *B*). (Scale bars: 5 μm.) (*C* and *D*) Seedling development when germinated on plates containing TIBA (25 μM, *C*) and jasplakinolide (10 μM, *D*). (*E–G*) Auxin translocation as monitored by auxin-responsive *DR5rev*::*GFP* expression after 4-h gravistimulation on plates containing solvent (*E*), TIBA (*F*), and jasplakinolide (*G*). (*H*) Effects of TIBA and jasplakinolide on cellular efflux of auxin (NAA) and benzoic acid (BeA) from *Arabidopsis* cultured cells, shown in the 30 min after addition of radiolabeled NAA or BeA. (*I* and *J*) Equivalent presence of PM-localized PIN1-GFP in control (*I*) and TIBA-treated (10 μM for 30 min) (*J*) tobacco BY-2 cells. (Scale bars: 10 μm.) Note that under the same conditions, TIBA effectively inhibits auxin efflux in *Arabidopsis* cells.

containing vesicles (SI Movie 13) has been blocked by both jasplakinolide (data not shown) and TIBA (SI Movie 14). Thus, it appears that after treatments with ATIs or jasplakinolide, even PM-resident PINs are less efficient in performing auxin efflux. This highlights the importance of actin-dependent PIN dynamics for the maintenance of auxin efflux.

Discussion

The transport-dependent asymmetric distribution of the plant hormone auxin represents a unique and widely operational mechanism by which plants integrate multiple signals and translate them into various developmental responses (1). For decades, various inhibitors of polar auxin transport have been essential tools in the formulation of these concepts (8). However, only little insight into the mechanism of their action has been gained. In this regard, our observations provide three important outcomes. (*i*) They show that ATIs, by affecting actin dynamics, inhibit subcellular vesicle trafficking processes. (*ii*) They demonstrate that ATIs are effective not only in plant cells but also in yeast and mammals, thus suggesting an evolutionary conserved target. (*iii*) They extend our knowledge about the cellular mechanism of polar auxin transport in plants, highlighting the importance of actin-based dynamics for this process.

ATIs Act as Actin Stabilizers in Eukaryotic Cells. As demonstrated here, prominent ATIs such as TIBA and PBA interfere with various cellular processes such as endocytosis and vesicle and organelle movements in plants. More specific effects of ATIs in mammalian cells on pinocytosis, endosomal movement at the cell periphery, and on dynamic movement of lamellipodia and mobility of fibroblasts suggest a link to the actin cytoskeleton because all of these processes depend strongly on a functional actomyosin system (25). Indeed, treatment with ATIs leads to increased bundling of actin and inhibition of actin dynamics in plant, yeast, and animal cells. Importantly, ATIs stabilize actin cytoskeleton even in the presence of actin-depolymerizing agents, further demonstrating that ATIs act on actin stabilization.

A recent study (36) has shown effects of different auxins and ATIs on meristem development in *Arabidopsis* roots. These long-term effects (48 h), which involve a more complex reprogramming of cellular behavior, also included changes in actin morphology. These observations, however, do not seem to be related to the rapid effects on actin dynamics reported here because in the long-term assays both ATIs and auxins are effective, which is in strong contrast to the direct, short-term effects of TIBA and PBA.

Notably, some established ATIs such as NPA do not show effects on subcellular dynamics (refs. 13 and 37 and our unpublished observations). Because the original identification of ATIs (some of which are chemically divergent) was based primarily on their ability to interfere with auxin transport-dependent physiological processes such as root gravitropism (34), it is not surprising that some ATIs may have different modes of action. Despite some reports suggesting an association of NPA with the actin cytoskeleton (38), and others showing that actin bundling enhances sensitivity to NPA (39), its mode of action does not seem to be related to the actin stabilization as we found for TIBA or PBA.

An unexpected outcome of the studies presented here was the potency of ATIs in nonplant systems such as yeast and mammalian cells, which further underlines a common target of these drugs in an evolutionary conserved process such actin dynamics. Because actin or myosin does not seem to be the direct target of ATIs, the molecular identity of the target remains a topic for future studies.

The Role of Actin-Based Vesicle Trafficking in the Mechanism of Polar Auxin Transport. Previous observations that the prominent components of auxin efflux and influx (PIN and AUX1 proteins, respectively) undergo constitutive cycling between the PM and endosomes (13–15) are hard to reconcile with classical models of auxin transport, which take into account only the cell surface-located auxin carriers (40). The roles of actin-dependent constitutive cycling of PIN and AUX1 transport components may be multiple. For example, it has been shown that constitutive cycling of PINs is used in a feedback manner to regulate auxin efflux by auxin itself (41). Another role of subcellular dynamics may be related to the rapid changes in the polarity of PIN localization as observed, for example, during gravitropism (42). Interestingly, actin stabilization by ATIs blocks PIN subcellular dynamics without affecting PIN polarity (13, 36) and still impairs auxin efflux out of cells and auxin transport in general. Furthermore, interference with actin dynamics also has an effect on auxin efflux in poorly polarized cultured cells, which suggests that actin-dependent constitutive cycling of auxin transport components might play a more fundamental role in the mechanism of auxin efflux. In such a scenario, the effects of ATIs on subcellular trafficking would underlie their effect on auxin transport. An alternative scenario, which cannot be entirely ruled out, would be that some ATIs (such TIBA and PBA), aside from their effect on auxin transport, also have a target unrelated to actin dynamics.

It was unexpected that a general inhibition of endocytosis and subcellular dynamics by ATIs is reflected by rather specific effects on auxin transport-related development. We believe that other possible effects are masked because of the excessive sensitivity of the auxin transport machinery to the perturbations of intracellular

trafficking and to its pronounced importance in plant development. This interpretation, however, does not exclude that some physiological and developmental effects of ATIs and, in particular, of jasplakinolide, are consequences of actin stabilization and do not relate to the auxin transport-dependent processes.

In conclusion, our observations provide a cellular mechanism for the action of a subclass of ATIs showing that they act as actin stabilizers and dramatically inhibit vesicle motility. They extend the classical chemiosmotic hypothesis of auxin transport by highlighting the importance of actin cytoskeleton-mediated vesicle trafficking for auxin transport. They suggest that, in addition to the PM localization of auxin transport components, vesicle-mediated endocytic cycling is an integral part of the functioning of polar auxin transport machinery. Overall, these studies also illustrate how a common, evolutionary-conserved eukaryotic process of actin-based vesicle motility fulfils a plant-specific physiological role.

Materials and Methods

Plant Material and Growth Conditions. *Arabidopsis* seedlings (Columbia ecotype) were grown on vertical agar plates at 25°C for 5 days. *Arabidopsis* lines transformed with ST-YFP (43), GFP-Ara7 (16), *DR5rev*::*GFP* (4), GFP-Fimbrin (29), and AIP1 RNAi (32) have been described before. Tobacco BY-2 suspension cells were grown, transformed with GFP-Ara7, ST-YFP, GFP-Fimbrin, and PIN1::PIN1-GFP, and maintained as described (16, 37). PGP1::PGP1-GFP and PGP19::PGP19-GFP constructs were created by C-terminal fusion of GFP to the cDNA of PGP1 and PGP19 and stably transformed into *Arabidopsis thaliana* (Col-0). Gravitropism analysis was performed as described in ref. 41.

Inhibitor Treatments in Plants. Two milliliters of 4-day-old BY-2 cell suspension or 15 *Arabidopsis* seedlings were incubated in respective 1 ml of liquid growth medium containing inhibitor or equal amounts of solvents (controls). Brefeldin A (Molecular Probes), TIBA (Duchefa), NPA (Duchefa), PBA (OlChemIm), BeA (Duchefa), latrunculin A and B (Sigma), and jasplakinolide (Molecular Probes) were used from 50 mM, 50 mM, 200 mM, 30 mM, 1 M, 10 mM, 10 mM, to 2 mM DMSO stock solutions, respectively.

Auxin Efflux Assay. Accumulation of [^{3}H]NAA and [^{3}H]BeA (Institute of Experimental Botany, Prague, Czech Republic, specific radioactivity 25 Ci/mmol and 22 Ci/mmol, respectively) in *Arabidopsis* cultured cells has been measured as described in ref. 9. For jasplakinolide, 2-h pretreatment was used.

Microscopy. Live-cell analysis of *Arabidopsis* root tips or tobacco BY-2 suspension cells was carried out as described in ref. 16. Ultrastructure analysis of ultrathin sections obtained from high-pressure freeze substitution-based fixed samples was carried out as described in ref. 14. HeLa cells and fibroblasts were grown, transfected with various mentioned markers, and analyzed as described in ref. 44. For Rab5 distribution analysis, the fluorescent intensity of Rab5 at the cell periphery and at the cell center was measured and evaluated as a ratio of peripheral intensity to the central intensity.

ACKNOWLEDGMENTS. We thank B. Scheres, P. Hussey, D. Menzel, W. Michalke, A. Nakano, and M. Zerial for sharing material and J. Mravec for technical help. P.D. and J.F. were supported by the Volkswagen-Stiftung and also by an European Molecular Biology Organization (EMBO) long-term fellowship (P.D.) and the EMBO Young Investigator Program (to J.F.), and GA AS Grant IAA601630703 (to J.F.). I.G. and A.A. were supported by The Netherlands Organization for Scientific Research (Nederlandse Organisatie voor Wetenschappelijk Onderzoek Grant 016.026.003 and Aard-en Levenswtenschappen Grant 814.02.005). P.D. and T.W.J.G. were supported by The Netherlands Organization for Scientific Research (Nederlandse Organisatie voor Wetenschappelijk Onderzoek Stiching voor Fundamenteel Onderzoek der Materie–Aard-en Levenswtenschappen Grant 805.47.012). J.P., D.S., and E.Z. were supported by the Ministry of Education, Youth, and Sports of the Czech Republic (LC06034) and GA AS Grant KJB600380604. J.H. was supported by Grant 204/05/0838 and Institutional Research Concept AV0Z50200510. A.S. was supported by the Max Planck Society. M.T. and K.O. were supported by Special Coordination Funds for Promoting Science and Technology, the Ministry of Education, Culture, Sports, Science, and Technology of Japan and by Grant-in-Aid for Scientific Research on Priority Area. R.T. and L.A.M. were supported by Iniciativa Científica Milenio Grants P02-009-F and P06-065-F.

1. Tanaka H, Dhonukshe P, Brewer PB, Friml J (2006) Spatiotemporal asymmetric auxin distribution: A means to coordinate plant development. *Cell Mol Life Sci* 63:2738–2754.
2. Benkova E, *et al*. (2003) Local, efflux-dependent auxin gradients as a common module for plant organ formation. *Cell* 115:591–602.
3. Blilou I, *et al*. (2005) The PIN auxin efflux facilitator network controls growth and patterning in Arabidopsis roots. *Nature* 433:39–44.
4. Friml J, *et al*. (2003) Efflux-dependent auxin gradients establish the apical-basal axis of Arabidopsis. *Nature* 426:147–153.
5. Luschnig C, Gaxiola RA, Grisafi P, Fink GR (1998) EIR1, a root-specific protein involved in auxin transport, is required for gravitropism in Arabidopsis thaliana. *Genes Dev* 12:2175–2187.
6. Scarpella E, Marcos D, Friml J, Berleth T (2006) Control of leaf vascular patterning by polar auxin transport. *Genes Dev* 20:1015–1027.
7. Niedergang-Kamien E, Leopold AC (1957) Inhibitors of polar auxin transport. *Physiol Plant* 10:29–38.
8. Snyder WE (1949) Some responses of plants to 2,3,5-triiodobenzoic acid. *Plant Physiol* 24:195–206.
9. Petrasek J, *et al*. (2006) PIN proteins perform a rate-limiting function in cellular auxin efflux. *Science* 312:914–918.
10. Bennett MJ, *et al*. (1996) Arabidopsis AUX1 gene: A permease-like regulator of root gravitropism. *Science* 273:948–950.
11. Yang Y, Hammes UZ, Taylor CG, Schachtman DP, Nielsen E (2006) High-affinity auxin transport by the AUX1 influx carrier protein. *Curr Biol* 16:1123–1127.
12. Wisniewska J, *et al*. (2006) Polar PIN localization directs auxin flow in plants. *Science* 312:883.
13. Geldner N, Friml J, Stierhof YD, Jurgens G, Palme K (2001) Auxin transport inhibitors block PIN1 cycling and vesicle trafficking. *Nature* 413:425–428.
14. Dhonukshe P, *et al*. (2007) Clathrin-mediated constitutive endocytosis of PIN auxin efflux carriers in Arabidopsis. *Curr Biol* 17:520–527.
15. Kleine-Vehn J, Dhonukshe P, Swarup R, Bennett M, Friml J (2006) Subcellular trafficking of the Arabidopsis auxin influx carrier AUX1 uses a novel pathway distinct from PIN1. *Plant Cell* 18:3171–3181.
16. Dhonukshe P, *et al*. (2006) Endocytosis of cell surface material mediates cell plate formation during plant cytokinesis. *Dev Cell* 10:137–150.
17. Ueda T, Yamaguchi M, Uchimiya H, Nakano A (2001) Ara6, a plant-unique novel type Rab GTPase, functions in the endocytic pathway of Arabidopsis thaliana. *EMBO J* 20:4730–4741.
18. Boevink P, *et al*. (1998) Stacks on tracks: The plant Golgi apparatus traffics on an actin/ER network. *Plant J* 15:441–447.
19. Vida TA, Emr SD (1995) A new vital stain for visualizing vacuolar membrane dynamics and endocytosis in yeast. *J Cell Biol* 128:779–792.
20. Conner SD, Schmid SL (2003) Regulated portals of entry into the cell. *Nature* 422:37–44.
21. Nielsen E, Severin F, Backer JM, Hyman AA, Zerial M (1999) Rab5 regulates motility of early endosomes on microtubules. *Nat Cell Biol* 1:376–382.
22. Gasman S, Kalaidzidis Y, Zerial M (2003) RhoD regulates endosome dynamics through Diaphanous-related Formin and Src tyrosine kinase. *Nat Cell Biol* 5:195–204.
23. Lenart P, *et al*. (2005) A contractile nuclear actin network drives chromosome congression in oocytes. *Nature* 436:812–818.
24. Moulding DA, *et al*. (2007) Unregulated actin polymerization by WASp causes defects of mitosis and cytokinesis in X-linked neutropenia. *J Exp Med* 204:2213–2224.
25. Small JV, Resch GP (2005) The comings and goings of actin: Coupling protrusion and retraction in cell motility. *Curr Opin Cell Biol* 17:517–523.
26. Tominaga M, *et al*. (2003) Higher plant myosin XI moves processively on actin with 35 nm steps at high velocity. *EMBO J* 22:1263–1272.
27. Choidas A, *et al*. (1998) The suitability and application of a GFP-actin fusion protein for long-term imaging of the organization and dynamics of the cytoskeleton in mammalian cells. *Eur J Cell Biol* 77:81–90.
28. Ayscough KR (2005) Coupling actin dynamics to the endocytic process in Saccharomyces cerevisiae. *Protoplasma* 226:81–88.
29. Voigt B, *et al*. (2005) GFP-FABD2 fusion construct allows in vivo visualization of the dynamic actin cytoskeleton in all cells of Arabidopsis seedlings. *Eur J Cell Biol* 84:595–608.
30. Spector I, Shochet NR, Kashman Y, Groweiss A (1983) Latrunculins: Novel marine toxins that disrupt microfilament organization in cultured cells. *Science* 219:493–495.
31. Bubb MR, Senderowicz AM, Sausville EA, Duncan KL, Korn ED (1994) Jasplakinolide, a cytotoxic natural product, induces actin polymerization and competitively inhibits the binding of phalloidin to F-actin. *J Biol Chem* 269:14869–14871.
32. Ketelaar T, *et al*. (2004) The actin-interacting protein AIP1 is essential for actin organization and plant development. *Curr Biol* 14:145–149.
33. Sabatini S, *et al*. (1999) An auxin-dependent distal organizer of pattern and polarity in the Arabidopsis root. *Cell* 99:463–472.
34. Morris DA (2000) Transmembrane auxin carrier systems—dynamic regulators of polar auxin transport. *Plant Growth Regul* 32:161–172.
35. Robinson JS, Albert AC, Morris DA (1999) Differntial effects of brefeldin A, cycloheximide on the activity of auxin efflux carriers in Cucurbita pepo L. *J Plant Physiol* 155:678–684.
36. Rahman A, *et al*. (2007) Auxin, actin and growth of the Arabidopsis thaliana primary root. *Plant J* 50:514–528.
37. Petrasek J, *et al*. (2003) Do phytotropins inhibit auxin efflux by impairing vesicle traffic? *Plant Physiol* 131:254–263.
38. Muday GK, Hu S, Brady SR (2000) The actin cytoskeleton may control the polar distribution of an auxin transport protein. *Gravit Space Biol Bull* 13:75–83.
39. Maisch J, Nick P (2007) Actin is involved in auxin-dependent patterning. *Plant Physiol* 143:1695–1704.
40. Goldsmith MHM (1977) The polar transport of auxin. *Annu Rev Plant Physiol* 28:439–478.
41. Paciorek T, *et al*. (2005) Auxin inhibits endocytosis and promotes its own efflux from cells. *Nature* 435:1251–1256.
42. Friml J, Wisniewska J, Benková E, Mendgen K, Palme K (2002) Lateral relocation of auxin efflux regulator AtPIN3 mediates tropism in Arabidopsis. *Nature* 415:806–809.
43. Grebe M, *et al*. (2003) Arabidopsis sterol endocytosis involves actin-mediated trafficking via ARA6-positive early endosomes. *Curr Biol* 13:1378–1387.
44. Akhmanova A, *et al*. (2001) Clasps are CLIP-115 and -170 associating proteins involved in the regional regulation of microtubule dynamics in motile fibroblasts. *Cell* 104:923–935.